Warming response of peatland CO$_2$ sink is sensitive to seasonality in warming trends

M. Helbig [1✉], T. Živković[2], P. Alekseychik [3], M. Aurela [4], T. S. El-Madany [5], E. S. Euskirchen [6], L. B. Flanagan[7], T. J. Griffis[8], P. J. Hanson [9], J. Hattakka[4], C. Helfter [10], T. Hirano [11], E. R. Humphreys [12], G. Kiely[13], R. K. Kolka [14], T. Laurila [4], P. G. Leahy [13], A. Lohila [4,15], I. Mammarella [15], M. B. Nilsson [16], A. Panov[17], F. J. W. Parmentier [18,19], M. Peichl [16], J. Rinne [19,20], D. T. Roman [14], O. Sonnentag[21], E.-S Tuittila [22], M. Ueyama [23], T. Vesala[15], P. Vestin[19], S. Weldon [24], P. Weslien[25] and S. Zaehle [5]

Peatlands have acted as net CO$_2$ sinks over millennia, exerting a global climate cooling effect. Rapid warming at northern latitudes, where peatlands are abundant, can disturb their CO$_2$ sink function. Here we show that sensitivity of peatland net CO$_2$ exchange to warming changes in sign and magnitude across seasons, resulting in complex net CO$_2$ sink responses. We use multiannual net CO$_2$ exchange observations from 20 northern peatlands to show that warmer early summers are linked to increased net CO$_2$ uptake, while warmer late summers lead to decreased net CO$_2$ uptake. Thus, net CO$_2$ sinks of peatlands in regions experiencing early summer warming, such as central Siberia, are more likely to persist under warmer climate conditions than are those in other regions. Our results will be useful to improve the design of future warming experiments and to better interpret large-scale trends in peatland net CO$_2$ uptake over the coming few decades.

At northern latitudes (>45° N), air temperatures are increasing rapidly, with winter temperatures rising faster than summer temperatures[1]. Warming is not spatially and seasonally uniform, with some areas of North America and Eurasia even experiencing cooling trends in the fall since the early 2000s despite annual warming[2]. Peatlands at northern latitudes store large amounts of organic carbon[3] and are long-term carbon dioxide (CO$_2$) sinks[4,5] exerting a global climate cooling effect[6]. However, the current peatland net CO$_2$ sink strength is sensitive to warming[7]. Changes in net ecosystem exchange (NEE) of CO$_2$ result from changes in photosynthesis and respiration. Rising air temperatures can enhance or decrease photosynthesis and respiration differently through direct temperature effects and through indirect effects on, for example, phenology, vegetation structure and water-table depth[8–14]. After snowmelt, low subsurface peat temperatures limit microbial activity and thus soil respiration[15] while high light levels and water availability together with increasing air temperatures induce rapid onset of photosynthetic activity, particularly in *Sphagnum* mosses[16,17]. In the summer, ecosystem respiration in peatlands has been found

to be dominated by autotrophic (plant) rather than heterotrophic (soil) respiration[14], with the former probably being more sensitive to air temperature than to soil temperature variations. At the same time, increasing water-table depth can affect photosynthetic activity and respiration in peatlands[18]. Lower water tables probably have a negative effect on *Sphagnum* moss productivity and a negligible or positive effect on shrub productivity[19] while warmer soils and enhanced oxygen availability in the peat profile can increase soil respiration[20,21]. Compared with spring, fall subsurface peat temperatures are warmer[22], contributing to enhanced soil respiration[23] while reduced light levels limit the positive effect of temperature on photosynthesis[8]. The resulting warming impact of combined photosynthesis and respiration responses on the peatland net CO$_2$ sink strength and thus on globally important carbon-cycle feedbacks still remains elusive[7,24].

Findings from a whole-ecosystem experiment suggest that peatland CO$_2$ loss through respiration increases linearly with uniform year-round warming relative to ambient temperatures across a broad range of warming up to +9 °C, turning the peatland into a net

[1]Department of Physics and Atmospheric Science, Dalhousie University, Halifax, Nova Scotia, Canada. [2]Department of Biology, Dalhousie University, Halifax, Nova Scotia, Canada. [3]Bioeconomy and Environment, Natural Resources Institute Finland, Helsinki, Finland. [4]Finnish Meteorological Institute, Helsinki, Finland. [5]Department of Biogeochemical Integration, Max Planck Institute for Biogeochemistry, Jena, Germany. [6]Institute of Arctic Biology, University of Alaska Fairbanks, Fairbanks, AK, USA. [7]Department of Biological Sciences, University of Lethbridge, Lethbridge, Alberta, Canada. [8]Department of Soil, Water, and Climate, University of Minnesota, Saint Paul, MN, USA. [9]Oak Ridge National Laboratory, Oak Ridge, TN, USA. [10]UK Center for Ecology and Hydrology, Edinburgh, UK. [11]Research Faculty of Agriculture, Hokkaido University, Sapporo, Japan. [12]Department of Geography and Environmental Studies, Carleton University, Ottawa, Canada. [13]School of Engineering and Architecture and Environmental Research Institute, University College Cork, Cork, Ireland. [14]USDA Forest Service, Northern Research Station, Grand Rapids, MN, USA. [15]Institute of Atmospheric and Earth System Research, University of Helsinki, Helsinki, Finland. [16]Department of Forest Ecology and Management, Swedish University of Agricultural Sciences, Umeå, Sweden. [17]V. N. Sukachev Institute of Forest SB RAS, KSC SB RAS, Krasnoyarsk, Russian Federation. [18]Centre for Biogeochemistry in the Anthropocene, Department of Geosciences, University of Oslo, Oslo, Norway. [19]Department of Physical Geography and Ecosystem Science, Lund University, Lund, Sweden. [20]Production Systems Unit, Natural Resources Institute Finland, Helsinki, Finland. [21]Département de géographie, Université de Montréal, Montréal, Quebec, Canada. [22]School of Forest Sciences, University of Eastern Finland, Joensuu, Finland. [23]Graduate School of Agriculture, Osaka Metropolitan University, Osaka, Japan. [24]Division of Environment and Natural Resources, Norwegian Institute of Bioeconomy Research, Ås, Norway. [25]Department of Earth Sciences, University of Gothenburg, Gothenburg, Sweden. ✉e-mail: manuel.helbig@dal.ca
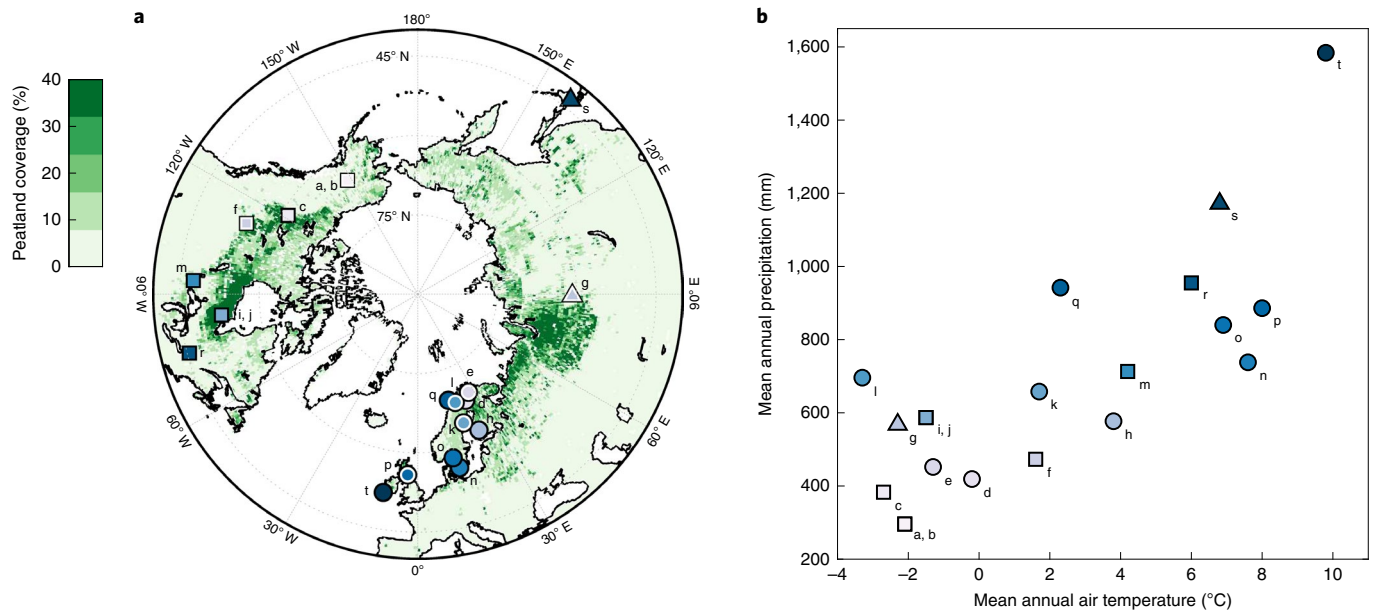
Fig. 1 | Spatial distribution and climatic conditions of studied peatland sites. a, Map of northern peatland extent (>45° N; data from ref. [3]) and location of multiannual (≥5 years) eddy covariance flux tower sites in northern peatlands (circles, squares and triangles). **b**, Mean annual air temperature and annual precipitation (1981–2010) across the 20 study sites (data from Climatic Research Unit (CRU) time series (TS) v.4.04). Squares, circles and triangles show sites in North America, Europe and Asia, respectively. Letters in **a** and **b** refer to sites listed in Supplementary Table 1.

CO_2 source in response to even a moderate warming treatment[25]. By contrast, historical air-temperature records reveal seasonal differences in warming trends[2,26] (Extended Data Fig. 1) that are not mimicked in most warming experiments[27]. In the field, 12 years of in situ observations have shown that annual and growing-season means of meteorological variables are only weak predictors of interannual variability of peatland NEE[28]. The weak relationships might be caused by small interannual temperature variability compared with warming experiments[25], by seasonally varying and compensating effects of peatland NEE sensitivity to temperature[29] or by complex interactions with other environmental drivers (for example, water table influencing phenology)[14]. For example, increased net CO_2 uptake in response to earlier snowmelt[30–32] and to warmer air temperatures in the early growing season has been observed in some peatlands[29,33,34]. Other studies report decreased net CO_2 uptake or even net CO_2 loss during periods of drier conditions with lower water-table positions, particularly in the late growing season[34–37]. During these periods, warmer air temperatures and increased atmospheric water demand[38] often coincide with below-normal precipitation inputs[39]. The highest net CO_2 losses have been found during periods when low peatland water-table positions co-occurred with warm air temperatures and increased evapotranspiration[38,40,41]. Despite their crucial importance for vegetation productivity and ecosystem respiration, indirect evapotranspiration, precipitation and water-table impacts are often poorly captured in warming experiments[37,42,43]. In natural peatlands, the sensitivity of the CO_2 sink strength to warming results from the combined effects of direct and indirect warming responses. Their contributions to NEE variation are expected to vary between seasons and when combined with seasonally varying warming trends can lead to diverging changes in CO_2 sink strength[8,29]. Thus, to better understand how seasonal warming responses contribute to peatland CO_2 sink changes on decadal timescales, we require long-term, multiannual, in situ field observations at the ecosystem scale. The results of long-term studies can help to advance our understanding of peatland carbon-cycle–climate feedbacks and can complement warming and water-table manipulation experimental plot-scale studies[12].

This study aims to better understand how spatially and seasonally heterogeneous warming affects the annual peatland net CO_2 sink. Our findings will help to determine whether peatlands will continue to exert a cooling impact on climate or will start exerting a warming impact on the global climate system over the next few decades. To quantify the effect of warmer air temperatures on interannual variability in annual and seasonal NEE, we analyse in situ, multiannual (≥5 years), ecosystem-scale NEE observations obtained with the eddy covariance technique from 20 northern peatland sites (194 site-years; Fig. 1 and Supplementary Table 1). First, we compare sensitivity of annual NEE anomalies (difference from mean annual NEE during observation period) with annual air-temperature anomalies derived from field observations and from a whole-ecosystem warming experiment with uniform year-round warming treatments between +2.25 °C and +9 °C relative to ambient conditions. Second, we empirically derive mean temperature sensitivities of peatland NEE anomalies for six different periods (early and late winter, spring, early and late summer, and fall classified on the basis of site-specific air-temperature seasonality; Supplementary Fig. 1) using linear mixed-effect models and relate temperature sensitivities to underlying drivers, including Enhanced Vegetation Index [EVI] as a proxy for vegetation productivity, water-table depth as a proxy for water availability and incoming short-wave radiation as a proxy for light availability/ photosynthetically active radiation. Third, we combine empirical monthly temperature sensitivities of NEE with monthly resolved observation-based air temperature change estimates (1981–2020 versus 1951–1980) across northern latitudes (>45° N) to quantify the effect of seasonal differences in warming on decadal changes in the peatland net CO_2 sink.

Weakly linked interannual NEE and temperature anomalies

Mean annual NEE across all sites was $-52 \pm 15\,\text{gC m}^{-2}\,\text{yr}^{-1}$ (± standard error; $n = 20$; net CO_2 uptake), which is similar to mean C accumulation rates over the past millennium derived from northern peatland profiles (ranging between 3 and $80\,\text{gC m}^{-2}\,\text{yr}^{-1}$) (ref. [4]). Mean interannual variability in NEE (mean standard deviation)
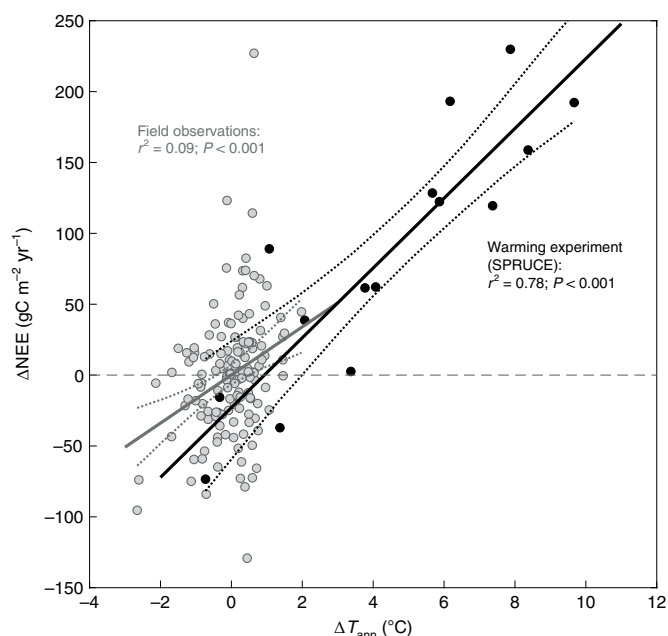
Fig. 2 | Relationship between annual air-temperature anomalies and annual peatland net CO_2 ecosystem exchange anomalies. Grey circles show the relationship between annual air-temperature anomalies (ΔT_{ann}) and annual peatland net CO_2 ecosystem exchange anomalies (ΔNEE) for 16 peatland sites with year-round observations for at least 5 years ($n=142$ site-years). Black circles show NEE anomalies and air-temperature anomalies from the Spruce and Peatland Responses Under Changing Environments (SPRUCE) whole-ecosystem warming experiment in northern Minnesota ($n=15$ site-years; differences are relative to mean NEE and air temperature of the ambient treatment (2016–2018) as reported by ref. [25]). Solid lines show ordinary least squares regressions, and the dotted lines indicate 95% CIs.

was $40\pm5\,\mathrm{gC\,m^{-2}\,yr^{-1}}$ ($\pm$ standard error; $n=20$) and amounted to 77% of mean annual NEE. Site means of annual net CO_2 uptake decreased with increasing latitude ($n=20$, $r^2=0.41$, $P<0.01$) with a slope of $5.4\,\mathrm{gC\,m^{-2}\,yr^{-1}}$ per degree latitude. However, site means of annual NEE were not related to mean annual air temperature ($P=0.42$) or annual precipitation ($P=0.33$). Instead, site means of annual net CO_2 uptake increased with increasing mean annual short-wave incoming radiation ($n=20$, $r^2=0.46$, $P<0.01$, slope $=-2.2\,\mathrm{gC\,m^{-2}\,yr^{-1}\,W^{-1}\,m^2}$; radiation data from ref. [44]), indicating light availability as an important control on latitudinal gradients in peatland net CO_2 uptake as already found in palaeoecological studies[4]. Mean annual air temperature across the observation sites ranged between $-3.3\,^{\circ}\mathrm{C}$ and $9.8\,^{\circ}\mathrm{C}$, and mean annual precipitation ranged between 296 mm and 1,584 mm (Fig. 1 and Supplementary Table 1). Peak mean monthly net CO_2 uptake was observed in June at 7 sites and in July at 13 sites. The timing of the largest mean monthly net CO_2 loss occurred between October and May, with the majority of the sites experiencing maximum net CO_2 loss in October and November ($n=11$).

The largest interannual variability of monthly NEE was observed in July while the largest interannual variability in monthly air temperatures was observed in December (Extended Data Fig. 2). Annual NEE anomalies across all sites and years were only weakly related to annual air-temperature anomalies ($r^2=0.09$; $P<0.001$; slope $=17.0$ (95% confidence interval (CI): 8.0–26.0) $\mathrm{gC\,m^{-2}\,yr^{-1}\,^{\circ}C^{-1}}$; $n=142$), indicating a slight decrease in net CO_2 uptake with higher mean annual air temperatures (Fig. 2). By contrast, about 80% of the variance in annual NEE anomalies at a whole-ecosystem warming

experiment in northern Minnesota[25] ($n=15$; $P<0.0001$) was explained by mean annual air-temperature anomalies across years and warming treatments (slope $=24.6$ (95% CI: 17.6–33.5) $\mathrm{gC\,m^{-2}\,yr^{-1}\,^{\circ}C^{-1}}$). At the warming experiment, the warming treatments resulted in a range of annual air-temperature anomalies more than twice as large ($10.4\,^{\circ}\mathrm{C}$) than the natural interannual variability at the observation sites in this study ($4.6\,^{\circ}\mathrm{C}$).

Seasonally asymmetric temperature responses of NEE

Relationships between monthly NEE and air-temperature anomalies changed over the course of the summer, with warmer early summers increasing net CO_2 uptake and warmer late summers decreasing net CO_2 uptake (Fig. 3a). During early and late winter, NEE response to warming was positive and small ($<0.3\,\mathrm{gC\,m^{-2}\,month^{-1}\,^{\circ}C^{-1}}$; that is, decreasing uptake with warming). Similarly, the shoulder seasons (spring and fall) showed decreasing uptake with warming with larger intersite variability than during the winter (as indicated by the 95% CI of the fixed-effects coefficient estimates). By contrast, increased net CO_2 uptake (negative regression slope) was observed for early summer months with $-1.6\,\mathrm{gC\,m^{-2}\,month^{-1}\,^{\circ}C^{-1}}$. The largest decrease in net CO_2 uptake with positive air-temperature anomalies was observed for the late summer months, with $+1.3\,\mathrm{gC\,m^{-2}\,month^{-1}\,^{\circ}C^{-1}}$. NEE sensitivity to near-surface soil-temperature ($<10\,\mathrm{cm}$) anomalies showed similar seasonal patterns as sensitivity to air-temperature anomalies (Supplementary Fig. 2), indicating that months with warmer air temperatures usually coincide with warmer near-surface soil temperatures (Supplementary Fig. 3). Differences in the magnitude of NEE responses could be explained by lower interannual soil-temperature variability compared with air temperature (Extended Data Fig. 3). For example, when warm air temperatures coincide with deep water tables, drier near-surface peat results in decreased soil thermal conductivity[45] and can attenuate heat transfer from the soil surface into the peat profile. The decreased heat transfer could explain lower interannual variability of soil temperature during the warmest months. The seasonal changes in NEE sensitivity highlight the contrasting responses across seasons, with warmer early summer conditions favouring mainly increased net CO_2 uptake, while warmer late summer conditions favour decreased net CO_2 uptake.

NEE sensitivity to EVI and water-table-depth anomalies

Increasing net CO_2 uptake with positive air-temperature anomalies in the early summer months coincided with the largest increase in net CO_2 uptake with positive EVI anomalies (higher vegetation productivity; Fig. 3b) while, in the later summer months, decreasing net CO_2 uptake with positive air-temperature anomalies was related to decreasing uptake with deeper water-table positions (drier conditions; Fig. 3c). At the same time, positive EVI anomalies still contributed to enhanced net CO_2 uptake. This pattern indicates enhanced vegetation productivity with warming (Supplementary Fig. 6b) is probably contributing to increased net CO_2 uptake in the early summer months while lower water tables are related to warmer air temperatures (Supplementary Fig. 6c) and decreased CO_2 uptake (Fig. 3c) in the late summer months. The shift in controls is further supported by the lower EVI sensitivity to air-temperature anomalies in the late compared with the early summer months (Supplementary Fig. 6b). Monthly water-table depth was positively correlated with air temperature for the late summer months but not for the early summer months, indicating deeper water tables in warmer years later in the summer (Supplementary Fig. 6c). The decreasing net CO_2 uptake with deepening water-table positions and with warmer air temperatures in the late summer months suggests that deeper water-table positions, and consequently a deeper oxic layer, lead to larger respiration rates and reduce the positive effect of warmer air temperatures on net CO_2 uptake. Net CO_2 uptake increased with positive incoming short-wave-radiation anomalies only in the fall
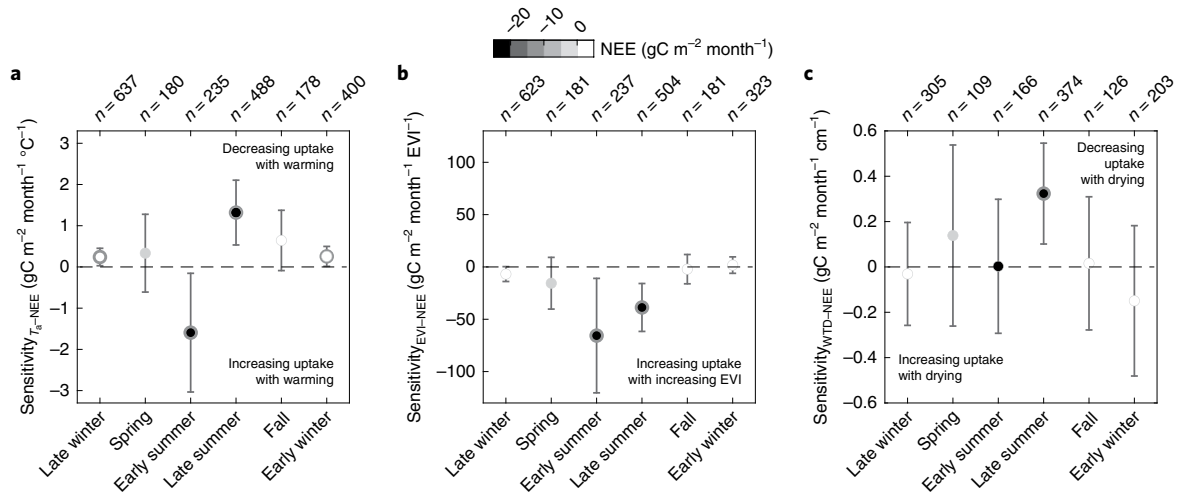
Fig. 3 | Sensitivities (regression slopes) between (ΔNEE) and environmental drivers in different seasons. a–c, Slopes of ΔNEE versus air-temperature anomalies (ΔT_a) (**a**), ΔNEE versus EVI anomalies (ΔEVI) (**b**) and ΔNEE versus water-table-depth anomalies (ΔWTD; positive ΔWTD indicates a deeper water table) (**c**) as derived from a linear mixed-effects regression model for six periods. Error bars show 95% CIs of estimated slope parameters, and bold circles indicate statistical significance at $\alpha \leq 0.05$. Mean NEE values are represented by the grey scale.

(Supplementary Fig. 4), indicating an enhanced net CO_2 sink during warm and cloudless fall periods, similar to previous findings for a peatland in northern Sweden[46]. However, NEE was not sensitive to incoming short-wave-radiation anomalies during spring and summer (absolute sensitivities of $<0.03\,gC\,m^{-2}\,month^{-1}\,(W\,m^{-2})^{-1}$ compared with $-0.14\,gC\,m^{-2}\,month^{-1}\,(W\,m^{-2})^{-1}$ in the fall). Similarly, reduced terrestrial CO_2 uptake during periods with reduced light availability in the late growing season has also been shown for other northern ecosystems[47]. Overall, we show that EVI, water-table depth and incoming short-wave radiation probably contribute to a large fraction of the observed NEE sensitivity to air-temperature anomalies. Their contributions vary throughout the seasons, with water-table depth being more important during the late summer months when vegetation productivity is usually light limited and warmer and drier soils favour high ecosystem respiration rates[8,48]. During the early summer months, EVI represents a major control on interannual NEE variability, probably due to enhanced gross primary productivity with warming-induced earlier vegetation greening[9].

**Seasonal warming differences and peatland NEE responses**

Seasonal warming trends have a substantial impact on estimated peatland NEE changes across northern latitudes (Fig. 4). We linked the monthly resolved temperature sensitivity of NEE (Extended Data Fig. 4) to monthly resolved observed warming between the periods 2001–2020 and 1951–1970 (Extended Data Fig. 1). NEE sensitivity to air-temperature anomalies shows a seasonal hysteresis, indicating differing peatland NEE responses to early summer warming compared with late summer warming (Extended Data Fig. 4 and Fig. 3a). When assuming seasonally uniform warming (same warming rate across all seasons), estimated changes in NEE scale linearly with warming rates, indicating a small decrease in peatland net CO_2 uptake between 1 and $12\,gC\,m^{-2}\,yr^{-1}$ (or 2–23% of current net CO_2 uptake) across the entire study area (Fig. 4b,d). When accounting for seasonally varying warming, the relationship between estimated change in annual peatland NEE and mean annual air-temperature change is more complex. The average decrease in net CO_2 uptake is approximately 30% smaller (with $4.6\,gC\,m^{-2}\,yr^{-1}$) than for seasonally uniform warming (with $6.6\,gC\,m^{-2}\,yr^{-1}$; Figs. 4a,c and 5). In some regions, such as central Siberia, where the largest early summer and smallest late summer warming is observed (Extended

Data Fig. 1), our simulation suggests the smallest NEE changes ($<0.5\,gC\,m^{-2}\,yr^{-1}$) despite annual warming rates of about 2°C (Fig. 4c). There, increased net CO_2 uptake occurring with warming in early summer months approximately balances losses occurring with warming in late summer and winter months, which is supported by in situ NEE observations[32]. The largest differences were observed for regions experiencing more than 2°C of June (early summer) warming (Extended Data Fig. 5) where the decrease in net CO_2 uptake was about 60% lower for seasonally varying warming (with $3.6\,gC\,m^{-2}\,yr^{-1}$) than for seasonally uniform warming (with $9.1\,gC\,m^{-2}\,yr^{-1}$). By contrast, in areas with less than 1°C of June warming, the decrease in net CO_2 uptake is similar between seasonally varying warming (with $4.6\,gC\,m^{-2}\,yr^{-1}$) and seasonally uniform warming (with $4.2\,gC\,m^{-2}\,yr^{-1}$). Accounting for seasonally varying warming is therefore crucial to accurately estimate future changes in peatland NEE.

Our results highlight how seasonally varying warming interacts with seasonally varying peatland NEE responses to temperature and how it contributes to interannual variability in peatland CO_2 sink strength under current climate conditions. Understanding peatland CO_2 sink responses to warmer air temperatures now and in more extreme futures is crucial to assess the efficacy of peatland restoration and conservation efforts and their potential to mitigate anthropogenic CO_2 emissions[49,50]. Peatland restoration can be an effective climate mitigation strategy only if their net CO_2 sink function can be maintained in the future under the pressure of climate change. On decadal timescales, regions in the northern latitudes that experience pronounced early summer warming (for example, Central Siberia) appear to be more resilient to climate warming regarding their peatland net CO_2 uptake function (Fig. 4c). At the same time, peatlands in regions that are susceptible to increasing aridity during the late summer months may experience decreasing net CO_2 uptake or even net CO_2 loss (Fig. 3c). However, on longer timescales from decades to centuries, when temperatures are expected to exceed the current historical records, changes in the net CO_2 sink strength may be non-linear due to slower changes in ecosystem processes and structure such as plant and microbial species and trait composition adjusting to new climate conditions[4]. Contemporary NEE observations or short-term manipulation experiments (<10 years) probably cannot capture these slow changes[51]. Similar to peatlands, other boreal and temperate ecosystems have been found to experience increased net
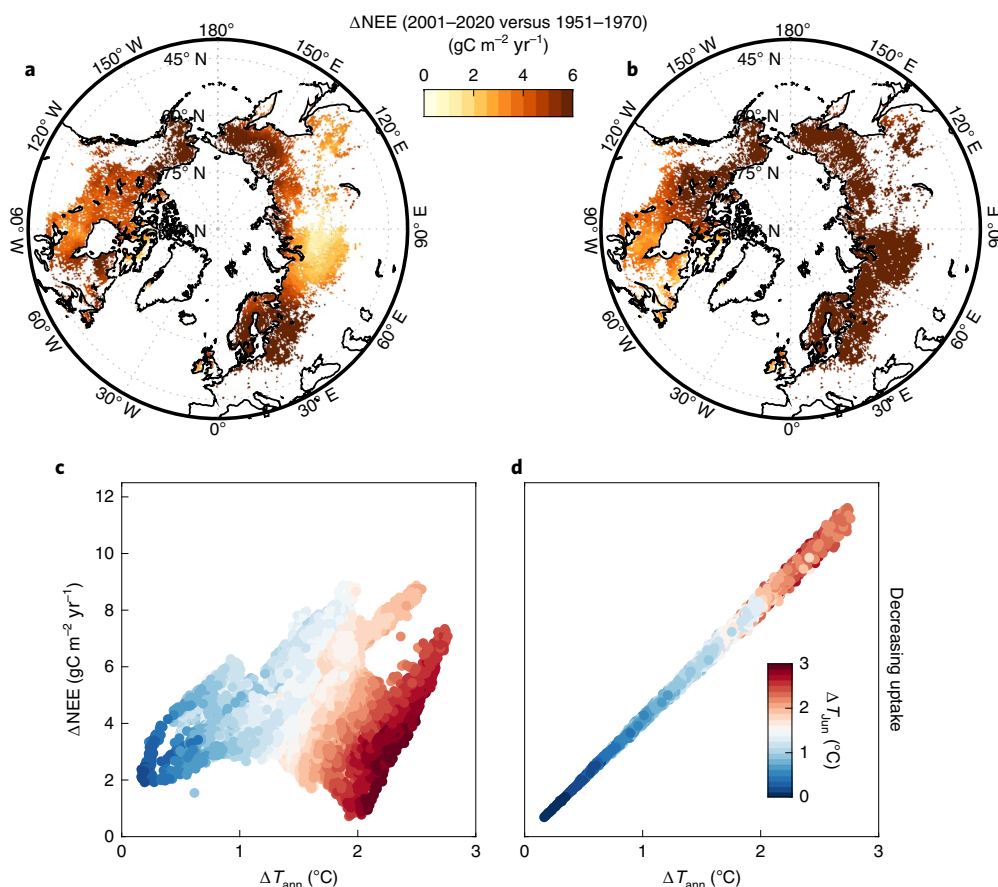
Fig. 4 | Estimated ΔNEE across northern latitudes (>45° N). a,b, Maps of ΔNEE (between the periods 1951–1970 and 2001–2020) for seasonally varying warming (**a**) and for seasonally uniform warming (**b**) (derived from CRU TS v.4.04). **c,d,** Relationship between change in annual air temperature (ΔT_{ann}) and ΔNEE for seasonally varying warming (**c**) and seasonally uniform warming (**d**). Differences between **c** and **d** result from differences in seasonal warming patterns. Circles indicate annual warming, while the colour scale represents mean June warming rates (ΔT_{Jun}). Each data point represents ΔNEE for one grid cell (0.5 × 0.5). Only grid cells with ≥5% peatland extent are shown.
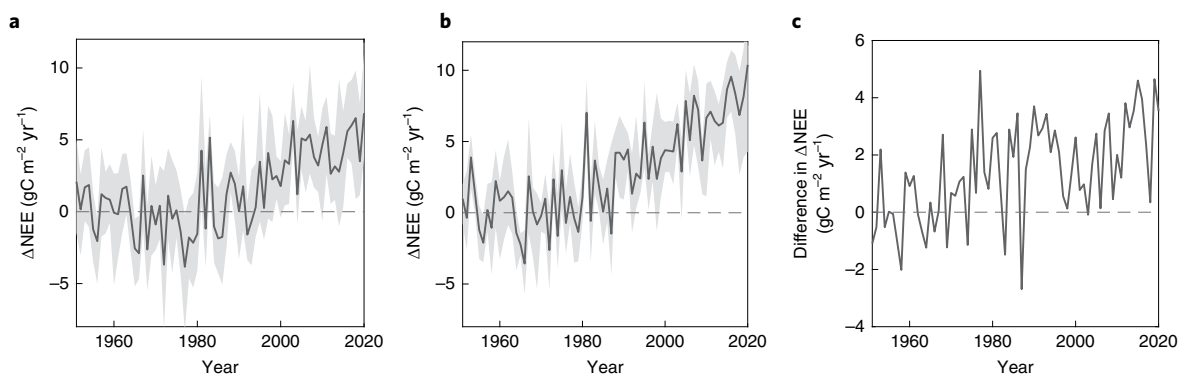
Fig. 5 | Annual time series of estimated ΔNEE. a–c, ΔNEE estimate for seasonally varying warming (**a**), for seasonally uniform warming (**b**) and for the difference between seasonally varying and seasonally uniform warming estimates (**c**). Solid lines show average ΔNEE for the study region, and the shaded area shows the 25th and 75th percentiles of ΔNEE (a measure of spatial variability). Estimated changes are relative to the period 1951–1970 considering seasonally varying temperature sensitivity of NEE. Only areas with ≥5% peatland extent are shown.

CO_2 uptake in response to warmer spring and early-growing-season temperatures and decreased uptake with warming in the late growing season and the related reductions in water availability and enhanced water stress[52–58]. In addition, atmospheric CO_2 concentration records have shown that since the late 1990s peak growing season, net CO_2 uptake across northern latitudes is increasing

with warmer air temperatures in the region[59]. We demonstrate that peatland NEE responses to interannual temperature variability show similar seasonal patterns. The results may partly explain why Siberia contributes more strongly to the increasing seasonality of atmospheric CO_2 concentration than North America over recent decades[60]. To better understand net CO_2 uptake responses of

northern peatland ecosystems, a concerted effort to continue existing observations of peatland NEE and to expand current coverage in regions of enhanced spring and early summer warming, such as central Siberia, is urgently needed. To conclude, we show that in addition to seasonal variations in peatland NEE response to warming, seasonal differences in warming itself play an important role for future changes in the northern peatland net CO_2 sink.

Online content

Any methods, additional references, Nature Research reporting summaries, source data, extended data, supplementary information, acknowledgements, peer review information; details of author contributions and competing interests; and statements of data and code availability are available at https://doi.org/10.1038/s41558-022-01428-z.

References

1. Xia, J. et al. Terrestrial carbon cycle affected by non-uniform climate warming. *Nat. Geosci.* **7**, 173–180 (2014).
2. Tang, R. et al. Increasing terrestrial ecosystem carbon release in response to autumn cooling and warming. *Nat. Clim. Change* **12**, 380–385 (2022).
3. Hugelius, G. et al. Large stocks of peatland carbon and nitrogen are vulnerable to permafrost thaw. *Proc. Natl Acad. Sci. USA* **117**, 20438–20446 (2020).
4. Gallego-Sala, A. V. et al. Latitudinal limits to the predicted increase of the peatland carbon sink with warming. *Nat. Clim. Change* **8**, 907–913 (2018).
5. Treat, C. C. et al. Widespread global peatland establishment and persistence over the last 130,000 y. *Proc. Natl Acad. Sci. USA* **116**, 4822–4827 (2019).
6. Frolking, S., Roulet, N. & Fuglestvedt, J. How northern peatlands influence the Earth's radiative budget: sustained methane emission versus sustained carbon sequestration. *J. Geophys. Res. Biogeosci.* **111**, G01008 (2006).
7. Loisel, J. et al. Expert assessment of future vulnerability of the global peatland carbon sink. *Nat. Clim. Change* **11**, 70–77 (2021).
8. Helbig, M. et al. Direct and indirect climate change effects on carbon dioxide fluxes in a thawing boreal forest–wetland landscape. *Glob. Change Biol.* **23**, 3231–3248 (2017).
9. Koebsch, F. et al. Refining the role of phenology in regulating gross ecosystem productivity across European peatlands. *Glob. Change Biol.* **26**, 876–887 (2020).
10. Huang, Y. et al. Tradeoff of CO_2 and CH_4 emissions from global peatlands under water-table drawdown. *Nat. Clim. Change* **11**, 618–622 (2021).
11. Evans, C. D. et al. Overriding water table control on managed peatland greenhouse gas emissions. *Nature* **593**, 548–552 (2021).
12. Helfter, C. et al. Drivers of long-term variability in CO_2 net ecosystem exchange in a temperate peatland. *Biogeosciences* **12**, 1799–1811 (2015).
13. Järveoja, J., Nilsson, M. B., Gažovič, M., Crill, P. M. & Peichl, M. Partitioning of the net CO_2 exchange using an automated chamber system reveals plant phenology as key control of production and respiration fluxes in a boreal peatland. *Glob. Change Biol.* **24**, 3436–3451 (2018).
14. Mäkiranta, P. et al. Responses of phenology and biomass production of boreal fens to climate warming under different water-table level regimes. *Glob. Change Biol.* **24**, 944–956 (2018).
15. Li, Q. et al. Abiotic and biotic drivers of microbial respiration in peat and its sensitivity to temperature change. *Soil Biol. Biochem.* **153**, 108077 (2021).
16. Moore, T. R. et al. Spring photosynthesis in a cool temperate bog. *Glob. Change Biol.* **12**, 2323–2335 (2006).
17. Korrensalo, A. et al. Species-specific temporal variation in photosynthesis as a moderator of peatland carbon sequestration. *Biogeosciences* **14**, 257–269 (2017).
18. Weltzin, J. F. et al. Response of bog and fen plant communities to warming and water-table manipulations. *Ecology* **81**, 3464–3478 (2000).
19. Dimitrov, D. D., Grant, R. F., Lafleur, P. M. & Humphreys, E. R. Modeling the effects of hydrology on gross primary productivity and net ecosystem productivity at Mer Bleue bog. *J. Geophys. Res. Biogeosci.* **116**, G04010 (2011).
20. Bubier, J., Crill, P., Mosedale, A., Frolking, S. & Linder, E. Peatland responses to varying interannual moisture conditions as measured by automatic CO_2 chambers. *Glob. Biogeochem. Cycles* **17**, 1066 (2003).
21. Moore, T. R. & Knowles, R. The influence of water table levels on methane and carbon dioxide emissions from peatland soils. *Can. J. Soil Sci.* **69**, 33–38 (1989).
22. Nichols, D. S. Temperature of upland and peatland soils in a north central Minnesota forest. *Can. J. Soil Sci.* **78**, 493–509 (1998).
23. Bellisario, L. M., Moore, T. R. & Bubier, J. L. Net ecosystem CO_2 exchange in a boreal peatland, northern Manitoba. *Écoscience* **5**, 534–541 (1998).
24. Yu, Z. et al. Peatlands and their role in the global carbon cycle. *Eos* **92**, 97–98 (2011).
25. Hanson, P. J. et al. Rapid net carbon loss from a whole-ecosystem warmed peatland. *AGU Adv.* **1**, e2020AV000163 (2020).
26. Vincent, L. A. et al. Observed trends in Canada's climate and influence of low-frequency variability modes. *J. Clim.* **28**, 4545–4560 (2015).
27. Templer, P. H. et al. Climate Change Across Seasons Experiment (CCASE): a new method for simulating future climate in seasonally snow-covered ecosystems. *PLoS ONE* **12**, e0171928 (2017).
28. Peichl, M. et al. A 12-year record reveals pre-growing season temperature and water table level threshold effects on the net carbon dioxide exchange in a boreal fen. *Environ. Res. Lett.* **9**, 055006 (2014).
29. Helbig, M., Humphreys, E. R. & Todd, A. Contrasting temperature sensitivity of CO_2 exchange in peatlands of the Hudson Bay Lowlands, Canada. *J. Geophys. Res. Biogeosci.* **124**, 2126–2143 (2019).
30. Griffis, T. J., Rouse, W. R. & Waddington, J. M. Interannual variability of net ecosystem CO_2 exchange at a subarctic fen. *Glob. Biogeochem. Cycles* **14**, 1109–1121 (2000).
31. Bubier, J. L., Crill, P. M., Moore, T. R., Savage, K. & Varner, R. K. Seasonal patterns and controls on net ecosystem CO_2 exchange in a boreal peatland complex. *Glob. Biogeochem. Cycles* **12**, 703–714 (1998).
32. Park, S.-B. et al. Temperature control of spring CO_2 fluxes at a coniferous forest and a peat bog in Central Siberia. *Atmosphere* **12**, 984 (2021).
33. Adkinson, A. C., Syed, K. H. & Flanagan, L. B. Contrasting responses of growing season ecosystem CO_2 exchange to variation in temperature and water table depth in two peatlands in northern Alberta, Canada. *J. Geophys. Res. Biogeosci.* **116**, G01004 (2011).
34. Heiskanen, L. et al. Carbon dioxide and methane exchange of a patterned subarctic fen during two contrasting growing seasons. *Biogeosciences* **18**, 873–896 (2021).
35. Lafleur, P. M., Roulet, N. T., Bubier, J. L., Frolking, S. & Moore, T. R. Interannual variability in the peatland-atmosphere carbon dioxide exchange at an ombrotrophic bog. *Glob. Biogeochem. Cycles* **17**, 1036 (2003).
36. Joiner, D. W., Lafleur, P. M., McCaughey, J. H. & Bartlett, P. A. Interannual variability in carbon dioxide exchanges at a boreal wetland in the BOREAS northern study area. *J. Geophys. Res. Atmos.* **104**, 27663–27672 (1999).
37. McVeigh, P., Sottocornola, M., Foley, N., Leahy, P. & Kiely, G. Meteorological and functional response partitioning to explain interannual variability of CO_2 exchange at an Irish Atlantic blanket bog. *Agric. For. Meteorol.* **194**, 8–19 (2014).
38. Helbig, M. et al. Increasing contribution of peatlands to boreal evapotranspiration in a warming climate. *Nat. Clim. Change* **10**, 555–560 (2020).
39. Bourgault, M.-A., Larocque, M. & Garneau, M. How do hydrogeological setting and meteorological conditions influence water table depth and fluctuations in ombrotrophic peatlands? *J. Hydrol. X* **4**, 100032 (2019).
40. Yurova, A., Wolf, A., Sagerfors, J. & Nilsson, M. Variations in net ecosystem exchange of carbon dioxide in a boreal mire: modeling mechanisms linked to water table position. *J. Geophys. Res. Biogeosci.* **112**, G02025 (2007).
41. Laine, A. M. et al. Warming impacts on boreal fen CO_2 exchange under wet and dry conditions. *Glob. Change Biol.* **25**, 1995–2008 (2019).
42. Chivers, M. R., Turetsky, M. R., Waddington, J. M., Harden, J. W. & McGuire, A. D. Effects of experimental water table and temperature manipulations on ecosystem CO_2 fluxes in an Alaskan rich fen. *Ecosystems* **12**, 1329–1342 (2009).
43. Juszczak, R. et al. Ecosystem respiration in a heterogeneous temperate peatland and its sensitivity to peat temperature and water table depth. *Plant Soil* **366**, 505–520 (2013).
44. Hao, D. et al. Estimating hourly land surface downward shortwave and photosynthetically active radiation from DSCOVR/EPIC observations. *Remote Sens. Environ.* **232**, 111320 (2019).
45. O'Donnell, J. A., Romanovsky, V. E., Harden, J. W. & McGuire, A. D. The effect of moisture content on the thermal conductivity of moss and organic soil horizons from black spruce ecosystems in interior Alaska. *Soil Sci.* **174**, 646–651 (2009).
46. Nijp, J. J. et al. Rain events decrease boreal peatland net CO_2 uptake through reduced light availability. *Glob. Change Biol.* **21**, 2309–2320 (2015).
47. Zhang, Y., Commane, R., Zhou, S., Williams, A. P. & Gentine, P. Light limitation regulates the response of autumn terrestrial carbon uptake to warming. *Nat. Clim. Change* **10**, 739–743 (2020).
48. Samson, M. et al. The impact of experimental temperature and water level manipulation on carbon dioxide release in a poor fen in northern Poland. *Wetlands* **38**, 551–563 (2018).
49. Drever, C. R. et al. Natural climate solutions for Canada. *Sci. Adv.* **7**, eabd6034 (2021).
50. Hemes, K. S., Runkle, B. R. K., Novick, K. A., Baldocchi, D. D. & Field, C. B. An ecosystem-scale flux measurement strategy to assess natural climate solutions. *Environ. Sci. Technol.* **55**, 3494–3504 (2021).

51. Walker, T. W. N. et al. A systemic overreaction to years versus decades of warming in a subarctic grassland ecosystem. *Nat. Ecol. Evol.* **4**, 101–108 (2020).

52. Xu, B. et al. Seasonal variability of forest sensitivity to heat and drought stresses: a synthesis based on carbon fluxes from North American forest ecosystems. *Glob. Change Biol.* **26**, 901–918 (2020).

53. Piao, S. et al. Net carbon dioxide losses of northern ecosystems in response to autumn warming. *Nature* **451**, 49–52 (2008).

54. Joyce, P. et al. How robust Is the apparent break-down of northern high-latitude temperature control on spring carbon uptake? *Geophys. Res. Lett.* **48**, e2020GL091601 (2021).

55. Grant, R. F. et al. Changes in net ecosystem productivity of boreal black spruce stands in response to changes in temperature at diurnal and seasonal time scales. *Tree Physiol.* **29**, 1–17 (2009).

56. Kwon, M. J. et al. Siberian 2020 heatwave increased spring CO_2 uptake but not annual CO_2 uptake. *Environ. Res. Lett.* **16**, 124030 (2021).

57. Yu, Z., Griffis, T. J. & Baker, J. M. Warming temperatures lead to reduced summer carbon sequestration in the U.S. Corn Belt. *Commun. Earth Environ.* **2**, 53 (2021).

58. Wang, S. et al. Warmer spring alleviated the impacts of 2018 European summer heatwave and drought on vegetation photosynthesis. *Agric. For. Meteorol.* **295**, 108195 (2020).

59. Wang, T. et al. Emerging negative impact of warming on summer carbon uptake in northern ecosystems. *Nat. Commun.* **9**, 5391 (2018).

60. Lin, X. et al. Siberian and temperate ecosystems shape Northern Hemisphere atmospheric CO_2 seasonal amplification. *Proc. Natl Acad. Sci. USA* **117**, 21079–21087 (2020).

Methods

Field- and satellite-based observations. In this study, we analysed multiannual (≥5 years) monthly NEE observations obtained with the eddy covariance technique at 20 northern peatland sites ($n = 2171$ site-months; Supplementary Table 1 (ref. [61])). Gap-filled NEE time series were synthesised from the literature and from open-access eddy covariance flux databases and were directly provided by flux tower principal investigators (Supplementary Table 1). NEE observations were aggregated to monthly totals for this study. Here we use the micrometeorological sign convention that negative NEE indicates net ecosystem CO_2 uptake and positive NEE indicates net ecosystem CO_2 loss to the atmosphere.

Air temperature ($n = 2,166$ site-months) and water-table depth ($n = 1,325$ site-months) were measured at the flux tower sites and were aggregated into monthly means. Monthly NEE, air-temperature and water-table-depth data from the literature were either directly extracted from tables or extracted using the online platform WebPlotDigitizer, version 4.1 (https://automeris.io/WebPlotDigitizer). In addition, we extracted mean annual air temperature and precipitation (1981–2010) from the gridded CRU TS v.4.05 climate database (0.5° x 0.5°) (ref. [62]) for each flux tower location (Supplementary Table 1 and Fig. 1).

Satellite-based monthly EVI ($n = 2,159$ site-months) was taken from the MODIS (moderate-resolution spectroradiometer) vegetation indices 16-day MOD13Q1 product (250 m resolution[63]) and used as a proxy for vegetation productivity[64]. The MOD13Q1 product covers the period 2000–2020, overlapping with most (>99%) of the NEE observation periods.

NEE responses to experimental warming and interannual variability. We compared the relationship between annual NEE and annual mean air-temperature anomalies from 16 northern peatland sites with ≥5 years of year-round observations ($n = 142$ site-years) with the relationship between annual NEE and annual mean air-temperature anomalies ($n = 15$) from a whole-ecosystem warming experiment in a forested bog in Minnesota, USA (data from ref. [25]). NEE anomalies for each peatland site were derived by subtracting the mean of the entire observation period at the specific site from the annual NEE values. At the warming experiment site, net ecosystem productivity was calculated by subtracting heterotrophic respiration from the sum of above-ground net primary productivity of trees, shrubs and *Sphagnum* mosses and below-ground net primary productivity. NEE was then taken as minus net ecosystem productivity in accordance with the micrometeorological sign convention. The warming experiment dataset covered the years 2016–2018 (1–3 years after warming began) for five different temperature treatments. Air- and soil-temperature treatments included +0 °C, +2.25 °C, +4.5 °C, +6.75 °C and +9 °C, and temperature differentials were applied uniformly throughout the year relative to ambient temperatures. Only data from treatments with ambient CO_2 concentrations were used in this study. Air-temperature and NEE anomalies were derived by subtracting the mean air temperature and NEE of the +0 °C treatment for the years 2016–2018, respectively.

NEE sensitivity to environmental drivers. We estimated NEE sensitivities to air temperature, water-table depth, vegetation productivity and incoming short-wave radiation anomalies for six different periods. Here we define sensitivities as the relationship between anomalies of monthly NEE sums and anomalies in the monthly mean of the respective explanatory variable. Periods were defined on the basis of standardized mean monthly air-temperature seasonality. For each site, the mean annual air temperature was subtracted from the mean monthly air temperatures and then divided by the standard deviation of monthly air temperatures to make seasonality comparable between sites with different temperature amplitudes (Supplementary Fig. 1). Spring and fall were defined for each site as the first and last months with a standardized air temperature above 0 °C, respectively. Early and later winter were defined as the months between fall and the month before minimum air temperature was reached and between the month with minimum air temperature and spring, respectively. Similarly, early and late summer were defined as the months between spring and the month before maximum air temperature was reached and between the month with maximum air temperature and fall, respectively. Snowmelt and snow onset dates could not be used to define periods since sites in Ireland and the United Kingdom did not experience an extended snow-cover period. To estimate NEE sensitivities for each period, we applied linear mixed-effects models using the fitlme and fixedEffects functions in Matlab (R2016a, TheMathWorks). The models were fitted to each response variable separately to characterize seasonal changes in NEE sensitivity to different driver variables. First, for each variable, monthly anomalies were derived by subtracting for each site the mean variable value for the corresponding month from the respective variable values. Second, the anomalies dataset was divided into the six different periods as described in the preceding. Last, for each period, a linear mixed-effects model was separately fitted for NEE anomalies, with fixed effects for monthly air temperature, water-table depth, EVI or incoming short-wave radiation anomalies and uncorrelated random effect for intercept and air temperature, water-table depth, EVI or incoming short-wave radiation anomalies grouped by site (similar to ref. [65]). Uncertainty intervals shown in Fig. 3 represent lower and upper 95% CIs for the respective fixed-effect coefficients. Water-table depth was available only for 18 sites, and water-table-depth time series for most sites were discontinuous, due mainly to winter soil frost.

Northern-latitude warming and simulated NEE responses. We used a historical gridded climate dataset to characterize seasonal differences in air-temperature warming rates across northern latitudes. Only areas with estimated peatland coverage of more than 5% were analysed (peatland extent data from ref. [3]). Monthly warming rates were calculated as the difference between mean monthly air temperatures for the periods 1951–1970 and 2001–2020 (data from CRU TS v.4.0[61]). Spatial resolution of the dataset was 0.5° × 0.5° and covered all land areas north of 45° N for this study. Mean monthly NEE temperature sensitivities across all peatland sites were derived by fitting linear mixed-effects models (see the preceding) to each month (Extended Data Fig. 4). To quantify the effect of seasonally varying warming on peatland NEE responses, the monthly NEE temperature sensitivity was multiplied by the warming rate for each month and grid cell. Annual NEE changes were then derived by summing monthly NEE changes from January to December. To quantify the effect of seasonally uniform warming, the monthly NEE temperature sensitivity was multiplied by the mean annual warming rate for each month and grid cell and then summed to annual NEE changes. To account for uncertainties in NEE sensitivity estimates, we ran a Monte Carlo simulation 1,000 times, randomly sampling for each run and for each month from a normal distribution around the mean monthly NEE sensitivities with a standard deviation equal to the standard error of the sensitivity estimate (derived using the fixedEffects function in Matlab (R2016a, TheMathWorks)). Then we took the median of the 1,000 NEE change estimates and compared median estimates from seasonally uniform and seasonally varying warming rates.

We note that this study analyses interannual variability over periods between 5 and 20 years. Decadal to centennial peatland NEE responses to continued warming are expected to be driven by long-term changes in vegetation structure and composition[66,67], which might not be fully captured by our analysis of interannual variability[51]. In addition, we tested whether the derived monthly NEE sensitivities to air-temperature anomalies are sensitive to the length of the observational time series. We found that seasonal patterns in NEE sensitivity are similar when comparing sensitivities derived only from sites with time series longer than 7 years ($n = 11$; Supplementary Table 1), derived from 5 yr subsets from all sites and derived from the full dataset (Supplementary Fig. 5).

Data availability

Monthly data used in this study can be accessed through the corresponding author's GitHub repository[61] (https://github.com/manuelhelbig/PeatlandNEE) and is available from the corresponding author upon request.

Code availability

All MATLAB code used in this study is made available through the corresponding author's GitHub repository[61] (https://github.com/manuelhelbig/PeatlandNEE). The software used to generate all results in this study is MATLAB 2016a.

References

61. Helbig, M. et al. Warming response of peatland CO_2 sink is sensitive to seasonality in warming trends. *Zenodo* https://doi.org/10.5281/zenodo.6685222 (2022).

62. Didan, K. *MOD13Q1 MODIS/Terra Vegetation Indices 16-Day L3 Global 250 m SIN Grid V006 [Data set]. NASA EOSDIS Land Processes DAAC* (2015); https://doi.org/10.5067/MODIS/MOD13Q1.006

63. Harris, I., Osborn, T. J., Jones, P. & Lister, D. Version 4 of the CRU TS monthly high-resolution gridded multivariate climate dataset. *Sci. Data* **7**, 109 (2020).

64. Lees, K. J. et al. Using spectral indices to estimate water content and GPP in *Sphagnum* moss and other peatland vegetation. *IEEE Trans. Geosci. Remote Sens.* **58**, 4547–4557 (2020).

65. Bennett, A. C., McDowell, N. G., Allen, C. D. & Anderson-Teixeira, K. J. Larger trees suffer most during drought in forests worldwide. *Nat. Plants* **1**, 15139 (2015).

66. Page, S. E. & Baird, A. J. Peatlands and global change: response and resilience. *Annu. Rev. Environ. Resour.* **41**, 35–57 (2016).

67. Juottonen, H. et al. Integrating decomposers, methane-cycling microbes and ecosystem carbon fluxes along a peatland successional gradient in a land uplift region. *Ecosystems* https://doi.org/10.1007/s10021-021-00713-w (2021).

Author contributions

M.H. designed the study. M.H. and T.Ž. developed the methodology. M.A., P.A., T.S.E.-M., E.S.E., L.B.F., T.J.G., J.H., C.H., T.H., E.R.H., G.K., R.K.K., T.L., P.G.L., A.L., I.M., M.B.N., A.P., F.J.W.P., M.P., J.R., D.T.R., O.S., E.-S.T., M.U., T.V., P.V., S.W., P.W. and S.Z. contributed eddy covariance flux data, and P.J.H. contributed data from the peatland warming experiment. M.H. analysed the data and wrote the first draft. All authors contributed to data interpretation and commented on the manuscript at all stages.

## Competing interests

Additional information
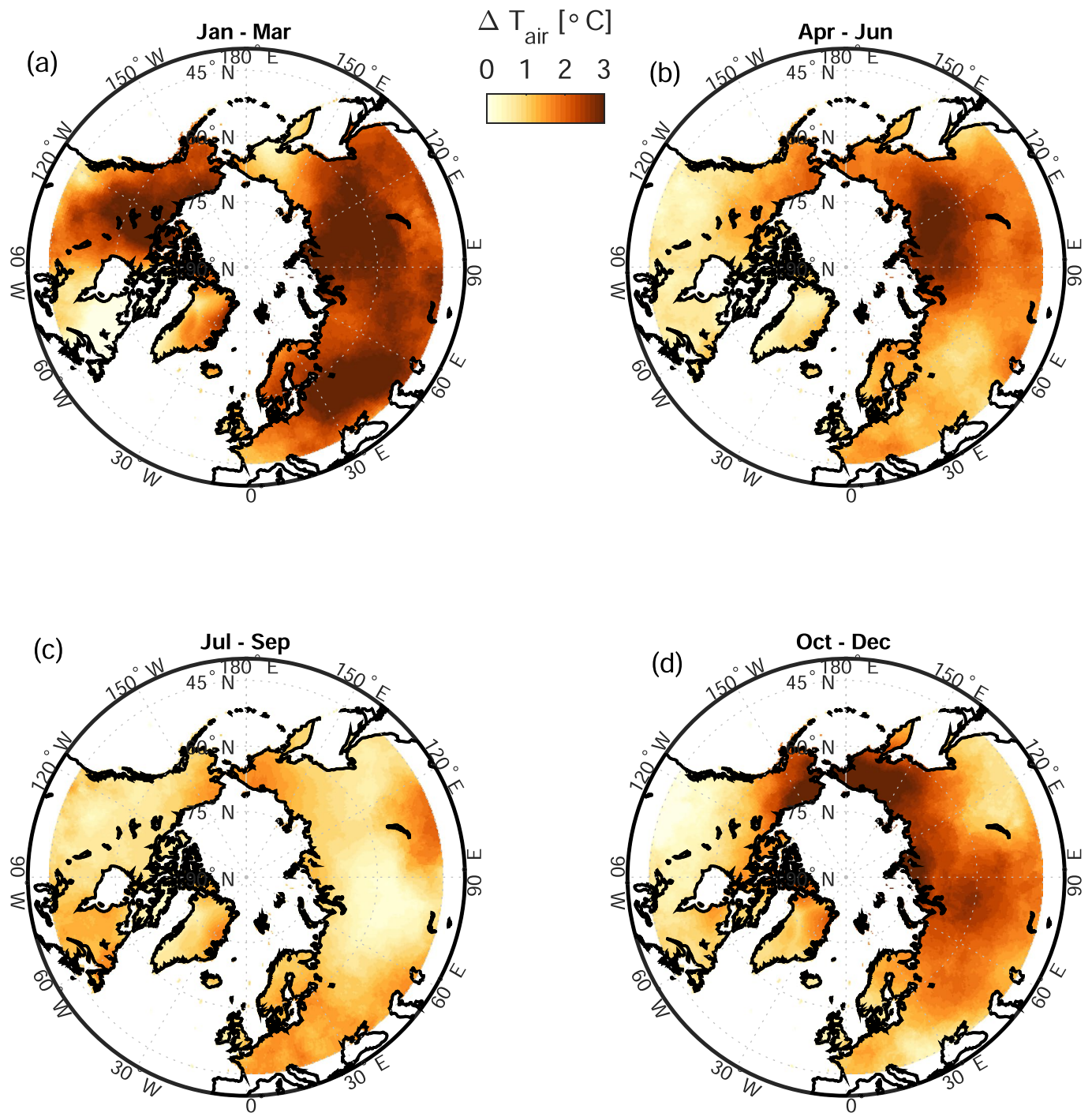
Extended Data Fig. 1 | Seasonal air temperature changes across northern latitudes. Warming rates across northern latitudes between 1951-1970 and 2001-2020 for **(a)** winter [January to March], **(b)** spring [April to June], **(c)** summer [July to September], and **(d)** fall [October to December] (data: CRU TS v4.0[61]).
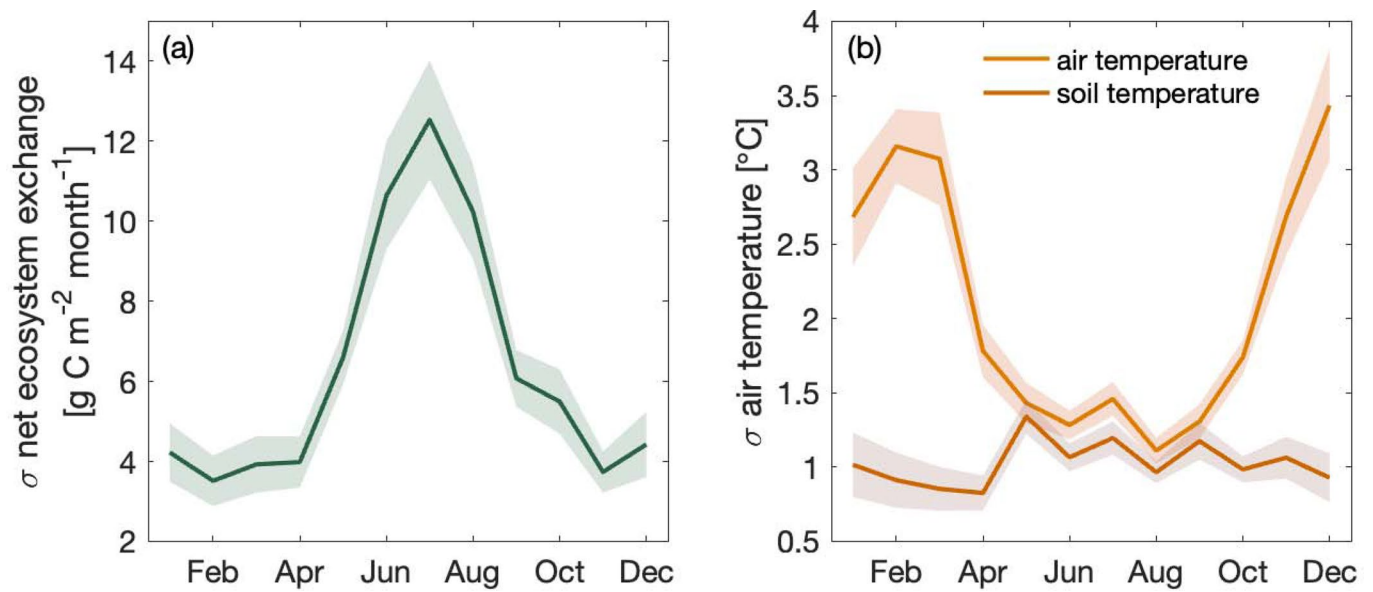
Extended Data Fig. 2 | Interannual variability of net ecosystem CO$_2$ exchange and air and soil temperature. Mean interannual variability in **(a)** net ecosystem CO$_2$ exchange (NEE) and **(b)** air and soil temperature across 20 peatland sites. Interannual variability is shown as the standard deviation of monthly NEE and air and soil temperature. Shaded areas show the standard error of the interannual variability across all sites.
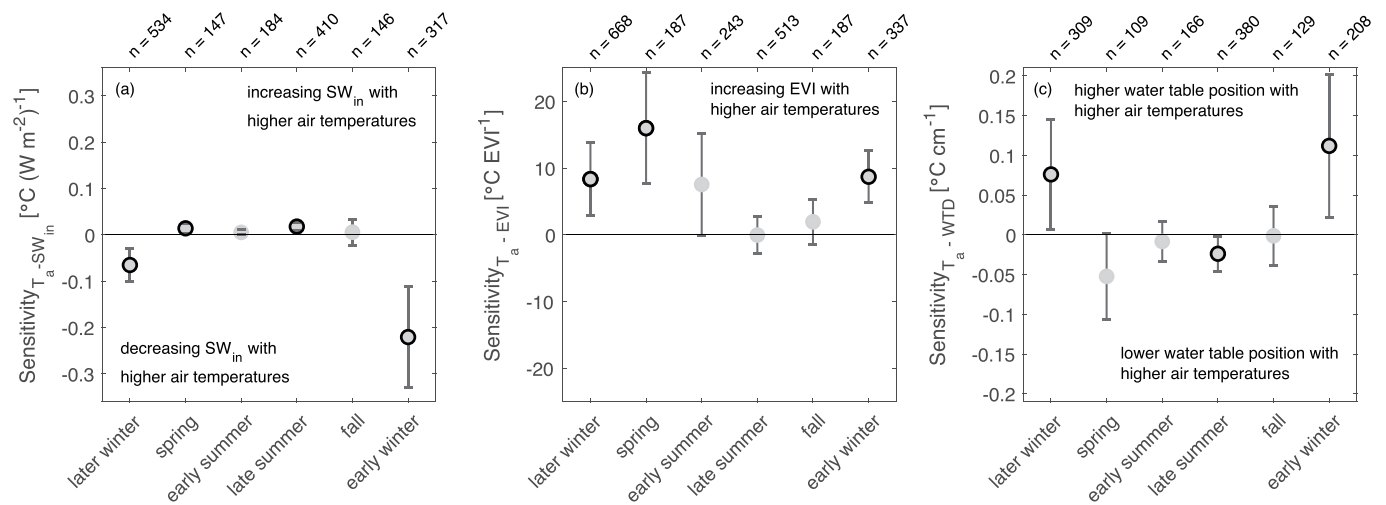
Extended Data Fig. 3 | Seasonal relationships between environmental drivers and air temperature. Estimated fixed effect (that is, monthly air temperature) slopes in linear mixed-effects regression models of **(a)** incoming shortwave radiation, **(b)** enhanced vegetation index [EVI], and **(c)** water table depth with sites as random effect. Linear mixed effect models are fitted separately to each period. Error bars show 95% confidence intervals of estimated slope parameters and black circles indicate statistical significance at $\alpha \leq 0.05$.
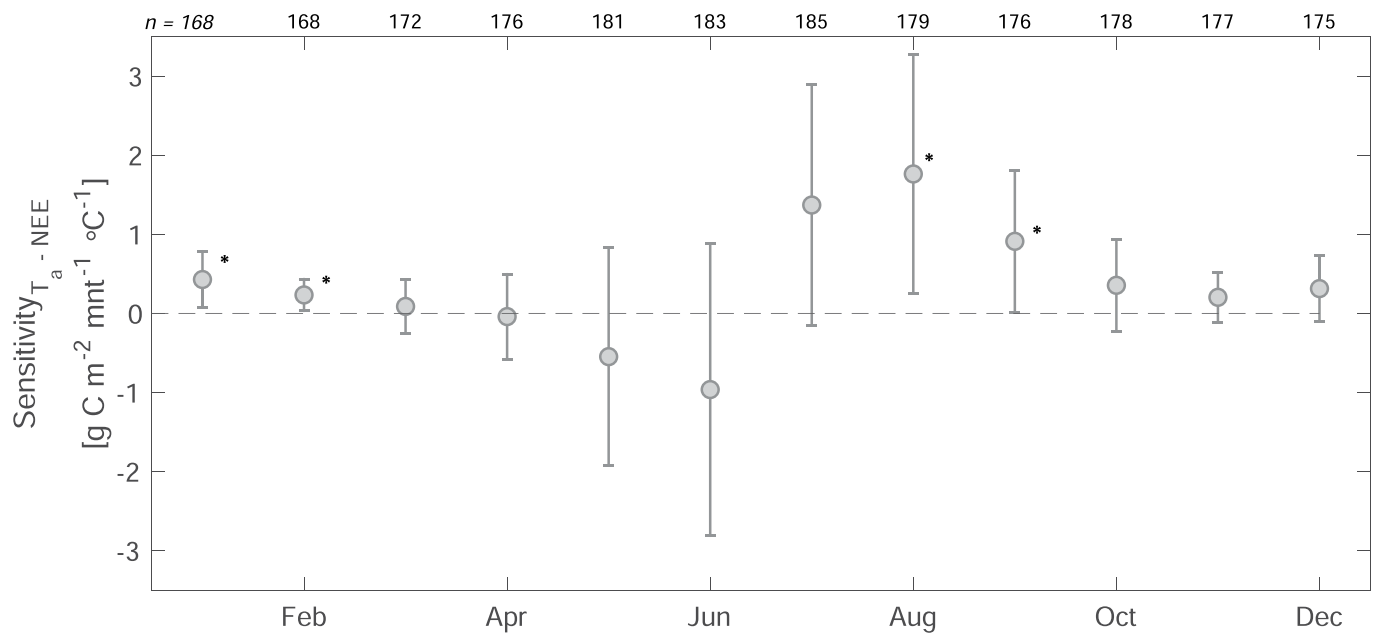
Extended Data Fig. 4 | Monthly relationships between air temperature and net ecosystem CO$_2$ exchange. Monthly estimated fixed effect (that is, monthly air temperature [T$_a$]) slopes in linear mixed-effects regression models of monthly net ecosystem CO$_2$ exchange (NEE) with sites considered as random effect. Asterisks indicate the level of statistical significance (* $p \leq 0.05$; ** $p \leq 0.01$; *** $p \leq 0.001$). The error bars represent the 95% confidence intervals of the estimated slope parameters.
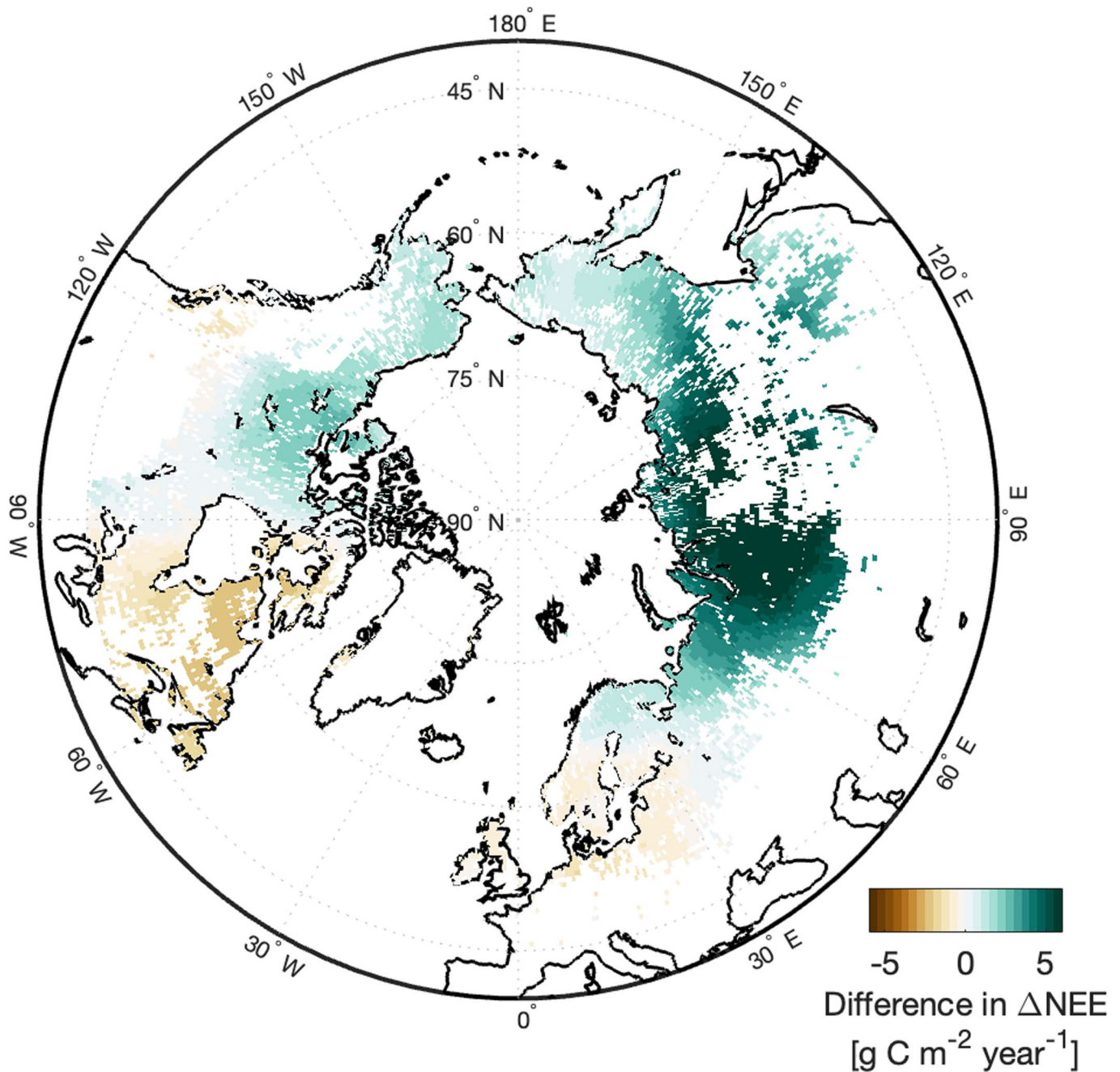
Extended Data Fig. 5 | Differences between seasonally varying and uniform warming impacts on net ecosystem CO_2 exchange. Differences in estimated change in annual peatland net ecosystem exchange (ΔNEE) between the period 1951 to 1970 and 2001 to 2020 resulting from seasonally varying and seasonally uniform warming for areas with $\geq$ 5% peatland extent. Green areas indicate larger net CO_2 loss for seasonally uniform warming and brown areas indicate smaller net CO_2 loss for seasonally uniform warming.